TECHNION RESEARCH AND DEVELOPMENT FOUNDATION LTD.

# MIXED STRATEGIES FOR THE INTERCEPTION OF "BLIND" HIGHLY MANEUVERING TARGETS

AFOSR Contract No. F61708-97-C0004

Annual Technical Report

covering the period of 1 September 1998 - 31 March 2000

Principal Investigator: Josef Shinar, Professor
Investigator: Tal Shima, Graduate Student



Faculty of Aerospace Engineering,
Technion, Israel Institute of Technology, Haifa, Israel.

# REPORT DOCUMENTATION PAGE

Form Approved OMB No. 0704-0188



| 1. AGENCY USE ONLY (Leave blank) | 2. REPORT DATE | 3. REPORT TYPE AND DATES COVERED |
|---|---|---|
| | 28-April-2000 | Final Report |

4. TITLE AND SUBTITLE

Mixed Strategies for the Interception of 'Blind' Highly Maneuvering Targets

5. FUNDING NUMBERS

F6170897C0004

6. AUTHOR(S)

Professor Josef Shinar

7. PERFORMING ORGANIZATION NAME(S) AND ADDRESS(ES)

Technion - Israel Institute of Science and Technology
Technion City
Haifa 32 000
Israel

8. PERFORMING ORGANIZATION REPORT NUMBER

N/A

9. SPONSORING/MONITORING AGENCY NAME(S) AND ADDRESS(ES)

EOARD
PSC 802 BOX 14
FPO 09499-0200

10. SPONSORING/MONITORING AGENCY REPORT NUMBER

SPC 97-4071

11. SUPPLEMENTARY NOTES

12a. DISTRIBUTION/AVAILABILITY STATEMENT

Approved for public release; distribution is unlimited.

12b. DISTRIBUTION CODE

A

13. ABSTRACT (Maximum 200 words)

This report results from a contract tasking Technion - Israel Institute of Science and Technology as follows: The contractor will validate previously developed strategies in a realistic three-dimensional variable speed environment. Analytical results will be compared with the results of 3-D nonlinear point-mass simulation. The validation will take place in three different scenarios as described in the proposal.

14. SUBJECT TERMS

EOARD, Mathematics, Missile Technology

15. NUMBER OF PAGES

34

16. PRICE CODE

N/A

| 17. SECURITY CLASSIFICATION OF REPORT | 18. SECURITY CLASSIFICATION OF THIS PAGE | 19. SECURITY CLASSIFICATION OF ABSTRACT | 20. LIMITATION OF ABSTRACT |
|---|---|---|---|
| UNCLASSIFIED | UNCLASSIFIED | UNCLASSIFIED | UL |

TECHNION RESEARCH AND DEVELOPMENT FOUNDATION LTD.

# MIXED STRATEGIES FOR THE INTERCEPTION OF "BLIND" HIGHLY MANEUVERING TARGETS

AFOSR Contract No. F61708-97-C0004

Annual Technical Report

covering the period of 1 September 1998 - 31 March 2000

Principal Investigator: Josef Shinar, Professor
Investigator: Tal Shima, Graduate Student

Faculty of Aerospace Engineering,
Technion, Israel Institute of Technology, Haifa, Israel.

## Table of contents

## Abstract

This Annual Technical Report, being the final report on a long-term investigation, has two objectives. It describes the technical effort performed in the last year and also summarizes the results of the entire (two and half years) investigation with an outline of the directions for future research.

Most missile guidance laws were developed using linearized two-dimensional models assuming constant speed and maneuverability. Simulation results demonstrated that linear guidance theory, based on such a model, couldn't predict the miss distance in an actual real world time-varying missile/target scenario, such as the interception of a reentering Tactical Ballistic Missile.

An earlier Interim Report described the first attempt to extend the linear guidance model to include time-varying speed and maneuverability. In this report the generalized time-varying linear pursuit-evasion game model is developed. Based on this model a modified guidance law with improved homing performance is derived. The predictions of the time-varying linear model are validated by simulations of a realistic Ballistic Missile Defense scenario.

Summarizing the more than two years investigation, it can be stated that its objective to gain an "understanding how key parameters in the models of the interceptor missile and of the target affect the outcome of an engagement" has been accomplished at least in a deterministic (noise free) environment. The affects of time-varying parameters and nonlinear kinematics were separately analyzed. Extension of the investigation to an environment corrupted by measurement noise, having been out of the scope of the reported effort from the outset, seems to be the appropriate direction for future research.

## Preface

This Annual Technical Report is in fact the final report on the investigation carried out at the Faculty of Aerospace Engineering in the Technion, Israel Institute of Technology, Haifa under AFOSR Contract No. F61708-97-C0004. The original contract was issued for one year starting on 17 August 1997, with an option to extend it to a second year. Actually, due to the unforeseen long hospitalization and the consecutive gradual return to work of the Principle Investigator, the research activities planned for the second year could not be completed in time and the contract was further extended until 31 March 2000.

The objective of the research contract was to the evaluation and development of interceptor guidance laws against highly maneuvering autonomous unmanned flying vehicles. The effort was aimed at understanding how key parameters in the models of the interceptor missile and of the target affect the outcome of an engagement.

Since the initiation of the research activities under the contract, several technical reports were submitted. In the first Interim Report the predictions of earlier studies, based on linear guidance theory, were compared to the results of three-dimensional point-mass simulations in realistic interception scenarios against tactical ballistic missiles. The main conclusions of linear guidance analysis were indeed confirmed, but the comparison also identified some discrepancies. The main discrepancies between the results of the nonlinear simulations in a realistic environment and linear guidance analysis were attributed to the affects of variable speed and maneuverability. In the selected anti-ballistic missile defense scenario the affect of nonlinear kinematics seemed to be secondary. These results were also presented at the AIAA 11$^{th}$ Multinational Conference on Theater Missile Defense, Monterey CA, June 1998 and the AIAA Guidance, Navigation and Control Conference, Boston, MA, August 1998.

The next report (Annual Technical Report 1998) concentrated on the affects of nonlinear kinematics. For this reason a point-defense scenario against highly maneuvering cruise missiles was analyzed. These results were presented at the AIAA Guidance, Navigation and Control Conference, Portland, OG, August 1999.

Based on the conclusions reached in the first year, the subsequent effort was aimed to extend the frequently used linear model to include known time-varying velocities and lateral acceleration bounds of the interceptor and target missiles. In the last Interim Report the first results of this effort were presented.

In this Annual Report the generalized time-varying linear pursuit-evasion game model is developed and its predictions are validated by simulations of a realistic Ballistic Missile Defense scenario. In addition to the description of this major technical effort, the results of the entire (two and half years) investigation effort are summarized and directions of some future research are outlined.

# PART 1

# TIME-VARYING LINEAR PURSUIT-EVASION GAME MODEL

## Notations

| | |
|---|---|
| **a** | acceleration |
| A | system matrix of the original system (19) |
| b | ballistic coefficient of the TBM |
| B | vector of the pursuer's control coefficients in the original system (20) |
| ***B*** | the pursuer's control coefficient in the transformed system (28) |
| C | vector of the evader's control coefficients in the original system (21) |
| ***C*** | the evader's control coefficient in the transformed system (29) |
| $C_D$ | drag coefficient |
| $C_L$ | lift coefficient |
| D | constant column vector (25) |
| $\mathcal{D}_0$ | *regular* region in the game space |
| $\mathcal{D}_1$ | *neutral* region in the game space |
| ***H*** | Hamiltonian (31) |
| J | cost function |
| m | mass |
| $M_s$ | guaranteed miss distance |
| n | load factor |
| S | reference area |
| t | time |
| T | thrust |
| $t_{go}$ | time to go |
| **u** | normalized pursuer control |
| V | velocity |
| **v** | normalized evader control |
| $x_i$ | state vector components (i = 1, 2, ... ,6) |
| X | vector of state variables of the original system (18) |
| y | distance of lateral separation |
| Z | zero effort miss distance (26), (61) |
| $\alpha$ | nondimensional acceleration |
| $\beta$ | nondimensional maneuverability change |
| $\Gamma$ | game dynamics (39) |

| | |
|---|---|
| $\varepsilon$ | target/interceptor time constant ratio |
| $\phi$ | aspect angle |
| $\Phi$ | transition matrix |
| $\theta$ | normalized time to go |
| $\lambda$ | co-state variable |
| $\Lambda$ | lift-to-drag ratio |
| $\mu$ | interceptor/target maneuverability ratio |
| $\sigma$ | line of sight angle |
| $\tau$ | autopilot time constant |

subscripts

| | |
|---|---|
| 0 | initial |
| b | burning |
| c | closing |
| E | evader (target) |
| f | final |
| P | pursuer (interceptor) |
| s | special value |
| x | longitudinal |

superscripts

| | |
|---|---|
| c | command |
| max | maximum |
| * | optimal |
| - | normalized |

abbreviations

| | |
|---|---|
| BMDO | Ballistic Missile Defense Organization |
| DGL | Differential Game Law |
| LOS | Line Of Sight |
| TBM | Tactical Ballistic Missile |

## Introduction

Interceptor missiles (either air-to-air or surface-to-air) were originally designed to destroy airplane targets. In spite of the well known fact that such scenario in general is characterized by nonlinear kinematics and time-varying velocities, most missile guidance laws were developed using linearized two-dimensional models assuming constant speed and maneuverability. It turned out that implementation of these guidance laws in a realistic environment has been nevertheless successful. The discrepancy between the simplified model and the complex reality has been expressed by the non-optimality of the guidance solution and the inaccurate prediction of the interception outcome.

In the first Interim Report of this contract, as well as in two subsequent conference papers [1, 2], the results derived from linearized guidance theory were compared to the outcome of three dimensional point mass simulations of interception scenarios against a highly maneuvering tactical ballistic missile (TBM). This comparison clearly showed that currently used linear guidance theory cannot predict well the miss distance in real world engagements.

In the scenarios evaluated in this works the interception end-game took place between 16-28 km of altitude. A typical velocity profile of the TBM and the interceptor are shown in Fig. 1. It can be seen that during the end-game the speed of the TBM remains almost unchanged, while the velocity of the interceptor is increasing. As a consequence, due to the larger air density in the lower altitudes, the maneuverability of the TBM is monotonically increasing. The design of the interceptor (carried out by a group of students after the Gulf War) has been aimed to keep the maneuverability in the end-game almost constant in spite of the increasing altitude and the resulting lower air density. The maneuverability profiles of both missiles are depicted in Fig. 2. Based on this data, the differences between the results derived from linearized guidance theory and the outcome of three dimensional point mass simulations has been attributed to the assumption of constant velocities and constant bounds on the lateral accelerations used in the linearized model. Moreover, it was found that due to the very high velocities the line of sight rotation, as well as the direction change of both missiles, remain small. Thus, the linearization of the trajectories with respect to the initial line of sight is a well-justified and valid approximation.

In the open technical literature there are several works that addressed the guidance problem of a variable speed missile [3-6]. None of this works proposed a model suitable to analyze the above-described TBM interception scenario. Thus, the need to develop a new linear time-varying interception model was established.

In the last Interim Report and a contemporary conference paper [7], the first results of this effort, extending the frequently used linear model to include known time-varying velocities and lateral acceleration bounds of the interceptor and target missiles, were presented. In the first part of this final report the generalized time-varying linear pursuit-evasion game model is developed and its predictions are validated by simulations of a realistic Ballistic Missile Defense scenario. In this model

the equations of motion remain linear, but the coefficients became time-varying. As in the earlier works [1, 2, 7] the interception scenario of a highly maneuvering TBM is formulated as a planar zero-sum pursuit-evasion game (the interceptor missile being the pursuer and the TBM the evader). The linear game model allows applying the method of "terminal projection", which reduces the dimension of the game dynamics and leads to a single state variable (the zero-effort miss distance). The new game solution has features similar to the previously used constant speed linear model, such as the decomposition of the state space into two regions etc., but the quantitative results are substantially different.

The structure of this part of the report is the following. In the next section the new linear time-varying model of the TBM interception is formulated. The general solution of this model is presented in the sequel. It is followed by the description of a simplified example with time varying target maneuverability and with time varying interceptor velocity. In the Appendix the solution of the game model with constant maneuverability and velocity [13] is repeated for sake of completeness.

## Problem Formulation

This report deals with time varying linear pursuit-evasion game models for realistic interception scenarios such as an endo-atmospheric interception of a maneuverable tactical ballistic missile (TBM). During the end-game of this interception scenario the altitude and the velocity of the reentering TBM, as well as of the interceptor missile, are continuously varying. Therefore their maneuverability is also changing. In this section a linear time-varying mathematical model of such an interception end-game is formulated. This planar model is based on the following set of assumptions:

(a-1) Both missiles can be represented by point-mass models with linear control dynamics.

(a-2) The relative end-game trajectory can be linearized around a fixed reference line such as the initial line of sight.

(a-3) The velocity profiles of both missiles on a nominal trajectory are known and can be expressed as the function of time.

(a-4) The maximum lateral acceleration of each missile is bounded by the maximum admissible angle of attack generating the highest available lift coefficient.

(a-5) The maneuvering dynamics of both missiles is approximated by first order transfer functions.

(a-6) The information structure is perfect.

The assumption of perfect information (a-6) has two parts: (i) the designers of both missiles have perfect knowledge of the engagement parameters; (ii) both missiles can accurately measure all the state variables. The second part (ii) is the "worst case" for the interceptor. In reality the TBM has no information on the interceptor's state variables, but it can maneuver randomly and has a non-zero probability to carry out a very close realization of the optimal deterministic interception avoidance strategy.

Typical velocity profiles for both missiles are shown in Fig. 1. Based on these profiles and assumption (a-3) the lateral acceleration bound of each missile can be computed (see Fig. 2) and expressed as the function of time (or time to go). In Fig. 3 a schematic view of the three-dimensional end-game geometry is shown. Note that the respective velocity vectors of the missiles are generally not aligned with the reference line. The angles $\phi_P$ and $\phi_E$ are, however, small. Thus, the approximations $\cos(\phi_i) \approx 1$, $\sin(\phi_i) \approx \phi_i$, $(i=P,E)$, are uniformly valid and coherent with (a-2). Nevertheless, the longitudinal accelerations of each missile have non-negligible components normal to the line of sight.

Based on (a-2) and (a-3) the final time of the interception can be computed for any given initial conditions of the end-game

$$t_f = \arg\{X_f = X_0 - \int_{t_0}^{t_f} [V_e(t) + V_p(t)]\, dt = 0\} \tag{1}$$

allowing to define the time-to-go by

$$t_{go} = t_f - t \tag{2}$$

The state variables in the equations of relative motion normal to the reference line are:

$$x_1 = y_e - y_p = y \tag{3}$$

$$x_2 = \dot{y} = V_e(t)x_6 - V_p(t)x_5 \tag{4}$$

$$x_3 = \mathbf{a}_P \tag{5}$$

$$x_4 = \mathbf{a}_E \tag{6}$$

$$x_5 = \phi_P \tag{7}$$

$$x_6 = \phi_E \tag{8}$$

The commanded lateral accelerations for each missile, $\mathbf{a}_P^c$ and $\mathbf{a}_E^c$, have maximum values that can be expressed as a function of time as $\mathbf{a}_p^{max}$ (t) and $\mathbf{a}_e^{max}$ (t) respectively. From the known velocity profiles $V_P(t)$ and $V_E(t)$ the respective longitudinal accelerations $\mathbf{a}_{xP}(t)$ and $\mathbf{a}_{xE}(t)$ can be computed and substituted into the equations of motion

$$\dot{x}_1 = x_2 \qquad ; x_1(0) = x_1^0 = 0 \tag{9}$$

$$\dot{x}_2 = x_4 - x_3 + \mathbf{a}_{xE}(t)\, x_6 - \mathbf{a}_{xP}(t)\, x_5 \qquad ; x_2(0) = x_2^0 \tag{10}$$

$$\dot{x}_3 = (\mathbf{a}_P{}^c - x_3)/\tau_P \qquad ; x_3(0) = x_3^0 \tag{11}$$

$$\dot{x}_4 = (\mathbf{a}_E{}^c - x_4)/\tau_E \qquad ; x_4(0) = x_4^0 \tag{12}$$

$$\dot{x}_5 = x_3/V_P(t) \qquad ; x_5(0) = x_5^0 \tag{13}$$

$$\dot{x}_6 = x_4/V_E(t) \qquad ; x_6(0) = x_6^0 \tag{14}$$

where

$$|\mathbf{a}_P{}^c| \le \mathbf{a}_P{}^{max}(t) \tag{15}$$

$$|\mathbf{a}_E{}^c| \le \mathbf{a}_E{}^{max}(t) \tag{16}$$

This set of equations can be summarized in a compact form as a linear, time dependent, vector differential equation

$$\dot{X} = A(t)\, X + B(t)\, \mathbf{u} + C(t)\, \mathbf{v} \tag{17}$$

with

$$X = (x_1, x_2, x_3, x_4, x_5, x_6)^T \tag{18}$$

$$A(t) = \begin{bmatrix} 0 & 1 & 0 & 0 & 0 & 0 \\ 0 & 0 & -1 & 1 & -a_{xP}(t) & a_{xE}(t) \\ 0 & 0 & -1/\tau_P & 0 & 0 & 0 \\ 0 & 0 & 0 & -1/\tau_E & 0 & 0 \\ 0 & 0 & 1/V_p(t) & 0 & 0 & 0 \\ 0 & 0 & 0 & 1/V_E(t) & 0 & 0 \end{bmatrix} \tag{19}$$

$$B(t) = \begin{bmatrix} 0 & 0 & a_P^{max}(t)/\tau_P & 0 & 0 & 0 \end{bmatrix}^T \tag{20}$$

$$C(t) = \begin{bmatrix} 0 & 0 & 0 & a_E^{max}(t)/\tau_E & 0 & 0 \end{bmatrix}^T \tag{21}$$

and the normalized controls

$$\mathbf{u} = \mathbf{a}_p{}^c/\mathbf{a}_p{}^{max}(t); \qquad |\mathbf{u}| \le 1 \tag{22}$$

$$\mathbf{v} = \mathbf{a}_E{}^c/\mathbf{a}_E{}^{max}(t); \qquad |\mathbf{v}| \le 1 \tag{23}$$

The natural cost function of the perfect information game is the miss distance

$$J = |D^T X(t_f)| = |x_1(t_f)| \tag{24}$$

where

$$D = (1, 0, 0, 0, 0, 0)^T \tag{25}$$

By using $\Phi(t_f, t)$, the well known transition matrix of the original homogeneous system, the transformation of *terminal projection* is introduced

$$Z(t) = D^T \Phi(t_f, t)\, X(t) \tag{26}$$

The new scalar state variable Z has the physical interpretation of the *zero effort miss distance* and its explicit form is given in the sequel (61). This transformation allows reducing the vector equation (17) to a scalar dynamic equation in the form

$$\dot{Z} = \boldsymbol{B}(t_f, t)\, \mathbf{u} + \boldsymbol{C}(t_f, t)\, \mathbf{v} \tag{27}$$

where

$$\boldsymbol{B}(t_f, t) = D^T \Phi(t_f, t)\, B(t) \le 0 \tag{28}$$

and

$$\boldsymbol{C}(t_f, t) = D^T \Phi(t_f, t)\, C(t) \ge 0 \tag{29}$$

with the cost function of (24) expressed as

$$J = |Z(t_f)| \tag{30}$$

## General Game Solution

### Necessary conditions of optimality

The perfect information linear differential game with bounded controls, formulated by equations (27)-(30), is solved in this section in the most general form. It closely follows the ideas outlined in [9], where this problem was first addressed.

The Hamiltonian of the game is

$$\boldsymbol{H} = \lambda_z \left[\boldsymbol{B}(t_f, t)\, \mathbf{u} + \boldsymbol{C}(t_f, t)\, \mathbf{v}\right] \tag{31}$$

where $\lambda_z$ is the co-state variable satisfying

$$\dot{\lambda}_z = -\,\partial \boldsymbol{H}/\partial Z = 0 \tag{32}$$

$$\lambda_z(t_f) = \partial J/\partial Z|t_f = \text{sign}\,\{Z(t_f)\}; \qquad Z(t_f) \neq 0 \tag{33}$$

which means that

$$\lambda_z(t) = \text{sign}\,\{Z(t_f)\}; \quad Z(t_f) \neq 0 \tag{34}$$

as long as $\lambda_z(t)$ is continuous. This allows determining the optimal strategies as

$$\mathbf{u}^* = \arg\min \boldsymbol{H} = -\,\text{sign}\{\boldsymbol{B}(t_f, t)\, Z(t_f)\}\,; \qquad Z(t_f) \neq 0 \tag{35}$$

$$\mathbf{v}^* = \arg\max \boldsymbol{H} = \text{sign}\{\boldsymbol{C}(t_f, t)\, Z(t_f)\}\,; \qquad Z(t_f) \neq 0 \tag{36}$$

that yield, using (28) and (29)

$$\mathbf{u}^* = \mathbf{v}^* = \text{sign}\,\{Z(t_f)\}\,; \qquad Z(t_f) \neq 0 \tag{37}$$

Substituting (37) into (31) yields the optimized game dynamics

$$\dot{Z}^* = \Gamma(t_f, t)\,\text{sign}\{Z(t_f)\}\,; \qquad Z(t_f) \neq 0 \tag{38}$$

with

$$\Gamma(t_f, t) = [\boldsymbol{B}(t_f, t) + \boldsymbol{C}(t_f, t)] \tag{39}$$

**Game solution structure**

Integrating (38) backward from any end condition $Z(t_f)$ generates candidate optimal trajectories. Several different cases can occur.

**Case 1:** $\Gamma(t_f, t)$ does not change sign $\{\Gamma(t_f, t) > 0 \;\forall\; t \in [t_0, t_f)\}$

Two families of monotonic optimal trajectories with opposite signs can be generated, filling the entire game space (see Fig. 4). The two trajectory families intersect on the Z=0 axis, which serves as a *dispersal line,* dominated by the evader. In this case the optimal strategies (37) can be expressed in a state feedback form

$$\mathbf{u}^* = \mathbf{v}^* = \text{sign}\,\{Z\} \quad \forall \quad Z \neq 0 \tag{40}$$

and the value of the game is a function of the initial conditions.

$$J^*(Z_0, t_0) = |Z_0| + \int_{t_0}^{t_f} \Gamma(t_f, t)\,dt \tag{41}$$

An example for this case with $\mathbf{a}_p^{\max}(t) < \mathbf{a}_e^{\max}(t)$ can be found in [8].

**Case 2:** $\Gamma(t_f, t)$ does not change sign $\{\Gamma(t_f, t) = 0 \ \forall \ t \in [t_0, t_f)\}$

The entire game space is filled with optimal trajectories that are actually straight lines (see Fig. 5). In this case the optimal strategies (37) in all of the game space excluding the Z=0 axis can be expressed in a state feedback form

$$\mathbf{u}^* = \mathbf{v}^* = \text{sign}\{Z\} \quad \forall \quad Z \neq 0 \tag{42}$$

The Z=0 axis is a singular surface separating two regions with different value function gradients. On it the optimal evader's strategy is arbitrary while the pursuer has to match this strategy. The value of the game in all of the game space is a function of the initial conditions.

$$J^*(Z_0, t_0) = |Z_0| \tag{43}$$

To the best of the authors' knowledge this case has not been presented in works in the open literature.

**Case 3:** $\Gamma(t_f, t)$ does not change sign $\{\Gamma(t_f, t) < 0 \ \forall \ t \in [t_0, t_f)\}$

The optimal trajectory pair generated from the point $Z(t_f)=0$ with different signs separate the game space into two regions of different solutions (see Fig. 6). Outside of these two optimal boundary trajectories, denoted respectively by $Z^*_+$ and $Z^*_-$, there is the region of *regular* trajectories denoted by $\boldsymbol{D}_1$ where the solution is given by (40) and (41). The boundary trajectories themselves belong to $\boldsymbol{D}_1$. Inside the other region, defined by

$$|Z(t)| < Z^*_+(t) \tag{44}$$

and denoted by $\boldsymbol{D}_0$, the optimal strategies are arbitrary and the value of the game is constant.

$$J_0^*(Z_0, t_0) = 0 \tag{45}$$

Inside this region $\lambda_z(t)$, which represents the gradient of the value function, is identically zero. Thus, the game space is decomposed into three regions of different constant gradients (+1, -1, 0) separated by the two *semi-permeable* optimal boundary trajectories $Z^*_+$ and $Z^*_-$, which are the *singular* surfaces of the game.

An example for this case with $\mathbf{a}_p^{max}(t) > \mathbf{a}_e^{max}(t)$ can be found in [8].

**Case 4:** $\Gamma(t_f, t)$ changes its sign once $\begin{Bmatrix} \Gamma(t_f,t)<0 & t\in[t_0,t_s) \\ \Gamma(t_f,t)=0 & t=t_s \\ \Gamma(t_f,t)>0 & t\in(t_s,t_f) \end{Bmatrix}$

The optimal trajectories have an extremum at $t = t_s$. As a backwards generated optimal trajectory intersects the Z=0 axis, it ceases to be optimal because the change in sign{Z}. The two families of such trajectories define a *dispersal line* of the game dominated by the evader. The boundary trajectories $Z^*_+$ and $Z^*_-$ are the pair of optimal trajectories that reach the Z=0 axis tangentially at $t = t_s$ which is the solution of $\Gamma(t_f, t) = 0$. The two regions of the different game solutions shown in Fig. 7 are

$$\boldsymbol{D_1} = \{(Z,t)|\ |Z(t)| \geq Z^*_+(t) \cup t_f \geq t \geq t_s\} \tag{46}$$

$$\boldsymbol{D_0} = \{(Z,t)|\ |Z(t)| < Z^*_+(t) \cap t < t_s\} \tag{47}$$

In $\boldsymbol{D_1}$ equations (40) and (41) provide the game solution. In $\boldsymbol{D_0}$ the optimal strategies are arbitrary and the value of the game is constant.

$$J_0^*(Z_0,t_0) = \int_{t_s}^{t_f} \Gamma(t_f,t)dt \tag{48}$$

The boundary trajectories and the *dispersal line* {Z(t)=0 for $t_f \geq t \geq t_s$}, dominated by the evader, belong to $\boldsymbol{D_1}$. An example for this case can be found in [9].

**Case 5:** $\Gamma(t_f, t)$ changes its sign once $\begin{Bmatrix} \Gamma(t_f,t)>0 & t\in[t_0,t_s) \\ \Gamma(t_f,t)=0 & t=t_s \\ \Gamma(t_f,t)<0 & t\in(t_s,t_f) \end{Bmatrix}$

The two optimal trajectories generated from the point $Z(t_f)=0$ with different signs intersect again on the Z=0 axis at $t = t_c < t_s$ (assuming $t_c > t_0$) and enclose the $\boldsymbol{D_0}$ region (see Fig. 8). All other optimal trajectory pairs, terminating at different values of $|Z(t_f)| \neq 0$, will also intersect each other on the Z=0 axis at $t < t_c$ (if $t_f$ is large enough) creating an evader dominated *dispersal line* {Z(t)=0} for $t_c \leq t \leq t_0$. Inside $\mathcal{D}_0$ the optimal strategies are arbitrary and the value of the game is zero as given by (45). Equation (40) and (41) give the game solution everywhere else (*i.e.* in $\mathcal{D}_1$). This case was first introduced in [7].

Remarks

1) Other cases, where $\Gamma(t_f, t)$ changes its sign more than once, can also occur. These cases are out of the scope of the present report.

2) In a game model with constant velocities and constant bounds on the lateral acceleration, solved in the Appendix, the conditions for the different cases can be easily determined (see Table A-1).

**Explicit computation of Z**

In order to compute $\Gamma(t_f, t)$ for the present problem, (17)-(25), the *zero effort miss distance* is derived explicitly. Assuming zero controls (11) and (12) yield

$$x_3(t) = x_3(t_0)\ e^{-t/\tau_P} \tag{49}$$

$$x_4(t) = x_4(t_0)\ e^{-t/\tau_E} \tag{50}$$

Substituting (49) and (50) into (13) and (14), respectively, yields

$$x_5(t) = x_5(t_0) + x_3(t_0) I_P(t) \tag{51}$$

$$x_6(t) = x_6(t_0) + x_4(t_0) I_E(t) \tag{52}$$

where

$$I_P(t) = \int_0^{\Delta t} \frac{e^{-\zeta/\tau_p}}{V_p(t)} d\zeta \tag{53}$$

$$I_E(t) = \int_0^{\Delta t} \frac{e^{-\zeta/\tau_E}}{V_E(t)} d\zeta \tag{54}$$

The integrals (53) and (54) have an analytic form only for very special cases of $V_P(t)$ and $V_E(t)$, respectively. Otherwise they have to be computed numerically. Substituting (51) and (52) into (10) yields

$$x_2(t) = x_2(t_0) + x_3(t_0)\tau_p[e^{-t/\tau_p} - 1 - \Pi_P(t)] - x_4(t_0)\tau_E[e^{-t/\tau_E} - 1 - \Pi_E(t)] - x_5(t_0)\cdot \\ \cdot[V_P(t) - V_P(t_0)] + x_6(t_0)\cdot[V_E(t) - V_E(t_0)] \tag{55}$$

where

$$\Pi_P(t) = \int_0^{\Delta t} \frac{I_P(\zeta) a_{xP}(\zeta)}{\tau_P} d\zeta \tag{56}$$

$$\Pi_E(t) = \int_0^{\Delta t} \frac{I_E(\zeta) a_{xE}(\zeta)}{\tau_E} d\zeta \tag{57}$$

and (3) becomes

$$x_1(t)=x_1(t_0)+x_2(t_0)t-x_3(t_0)\tau_p{}^2\left[e^{-t/\tau_p}+t/\tau_p-1+III_P(t)\right]+$$
$$+x_4(t_0)\tau_E{}^2\cdot\left[e^{-t/\tau_E}+t/\tau_E-1+III_E(t)\right]- \qquad (58)$$
$$-x_5(t_0)\left[IV_P(t)-V_P(t_0)t\right]+x_6(t_0)\left[IV_E(t)-V_E(t_0)t\right]$$

where

$$III_P(t)=\int_0^{\Delta t}\frac{II_P(\zeta)}{\tau_P}d\zeta \qquad ; \qquad IV_P(t)=\int_0^{\Delta t}V_P(\zeta)d\zeta \qquad (59)$$

$$III_E(t)=\int_0^{\Delta t}\frac{II_E(\zeta)}{\tau_E}d\zeta \qquad ; \qquad IV_E(t)=\int_0^{\Delta t}V_E(\zeta)d\zeta \qquad (60)$$

Thus the *zero effort miss distance* of the problem is

$$Z(t)=x_1(t)+x_2(t)t_{go}-x_3(t)\tau_P^2\left[e^{-\frac{t_{go}}{\tau_P}}+\frac{t_{go}}{\tau_p}-1+III_P(t_{go})\right]+$$
$$+x_4(t)\tau_E^2\cdot\left[e^{-\frac{t_{go}}{\tau_E}}+\frac{t_{go}}{\tau_E}-1+III_E(t_{go})\right]-x_5(t)\left[IV_P(t_{go})-V_P(t)t_{go}\right]+ \qquad (61)$$
$$+x_6(t_0)\left[IV_E(t)-V_E(t)t_{go}\right]$$

After eliminating equal terms, the time derivative of (61) becomes

$$\frac{dZ}{dt}=a_P^{max}(t)\left[e^{-t_{go}/\tau_P}+t_{go}/\tau_P-1+III_P(t_{go})\right]u- \qquad (62)$$
$$-a_E^{max}(t)\left[e^{-t_{go}/\tau_E}+t_{go}/\tau_E-1+III_E(t_{go})\right]v$$

Substituting (37) into (62) yields the optimal game dynamics

$$\frac{dZ^*}{dt}=\Gamma(t_f,t)\cdot\text{sign}(Z) \quad \forall \quad Z\neq 0 \qquad (63)$$

where

$$\Gamma(t_f,t) = a_P^{max}(t)\left[e^{-\frac{t_{go}}{\tau_P}} + \frac{t_{go}}{\tau_P} - 1 + III_P(t_{go})\right]\tau_P$$
$$- a_E^{max}(t)\left[e^{-\frac{t_{go}}{\tau_E}} + \frac{t_{go}}{\tau_E} - 1 + III_E(t_{go})\right]\tau_E \qquad (64)$$

## Validation Study

### Scenario description

In the simulated scenario a single guided interceptor missile is launched against a reentering TBM of high maneuverability. This scenario was analyzed in great details [1, 2] and compared to a simplified linear model. The results of that analysis motivated the present study. The results presented in this paper were obtained by the simulation program and its main features are repeated here for the sake of completeness.

The simulation program consists of the following elements: three-dimensional nonlinear relative kinematics between two point-mass vehicles, point-mass dynamics of both flying vehicles, simplified guidance and control dynamics of each vehicle and a high-altitude standard atmospheric model. The simulations are carried out in a fixed Cartesian coordinate system, assuming flat non-rotating earth and no wind. The well-known equations of three-dimensional kinematics and point-mass dynamics of atmospheric flying vehicles are summarized in [10] and not repeated here.

For sake of simplicity a point defense scenario is considered, *i.e.* the interceptor missile is launched from the vicinity of the TBM's target. The initial position of the TBM is determined by assuming a non-maneuvering ballistic trajectory aimed at a fixed surface target. The initial position of the TBM also determines the vertical plane of reference. When the reentering TBM is detected, the defense system selects the desired altitude for interception and launches a guided missile towards the predicted point of impact at this altitude. In this study a nominal interception altitude of 22 km is selected. The velocity and maximum lateral acceleration profiles along the nominal (non-maneuvering) trajectory are plotted in Figs. 1 and 2, respectively.

The results presented in this report concentrate on the interception end-game, where a sequence of "hard" TBM maneuvers is assumed to take place. This end-game starts when the TBM crosses the altitude of 28 km and has an approximate duration of 3 sec. The initial TBM maneuver is commanded to a direction (either right or left) perpendicular to the vertical reference plane. The sequence is completed by a second maneuver, commanded to the opposite direction, after some time $\Delta t_{sw} \in [0,3.16]$ sec. The values of $\Delta t_{sw}$ vary between different simulation runs in steps of approximately 0.25 sec corresponding to steps of 500 m of altitude.

These type of end-game maneuver sequence were selected because both optimal control [11, 12] and differential game [8, 9, 13] theories predict that the optimal missile avoidance maneuver (aimed to maximize the miss distance) has such a

"bang-bang" structure. Moreover, these maneuvers with varying $\Delta t_{sw}$, represent adequately the ensemble of the *random* maneuver samples [2] that can be implemented by the designer of a TBM without the knowledge of the interception altitude. In the next subsections the specific guidance and control models of a maneuvering TBM and the interceptor missile are described.

**TBM model**

The reentering TBM is assumed to be a generic cruciform flying vehicle having some control surfaces to execute lateral maneuvers up to a given angle of attack $\alpha_{max}$ in non-rolling body coordinates. The relationship between the actual angle of attack and its commanded value is approximated by a first-order transfer function with a time constant $\tau_E \in [0.01,0.4]$ sec. The generic TBM used in this study is characterized by its ballistic coefficient (b=5000 kg/m$^2$), which determines the deceleration in the atmosphere and the lift to drag ratio $\Lambda \in [1.41, 2.83]$ at the angle of attack generating maximum lift.

**Interceptor Model**

The generic interceptor missile (designed by a group of students for high endo-atmospheric interception) has an aerodynamically controlled cruciform airframe and is assumed to be roll stabilized. It has a two stage solid rocket propulsion. Each rocket motor provides a constant thrust. After the "burn out" of the first stage the booster is separated and the second rocket motor is ignited. The maneuverability of the missile (its lateral acceleration and the corresponding load factor) is limited, in each of the two perpendicular planes of the cruciform configuration, by the maximum lift coefficient. It is assumed that the missile's auto-pilot can be represented by a first-order transfer function with a time constant $\tau_P \in [0.05, 0.4]$ sec. The parameters of the interceptor are summarized in Table 1.

| Parameter | $t_b$ [sec] | T [kN] | $m_0$ [kg] | $m_f$ [kg] | $SC_D$[m$^2$] | $SC_{Lmax}$ [m$^2$] |
|---|---|---|---|---|---|---|
| Stage 1 | 6.5 | 229.0 | 1540.0 | 933.0 | 0.10 | 0.24 |
| Stage 2 | 13.0 | 103.0 | 781.0 | 236.0 | 0.05 | 0.20 |

Table 1. Interceptor Data

The guidance system of the interceptor missile consists of two identical, de-coupled channels, associated with the perpendicular planes of the cruciform configuration. Since the missile is roll stabilized, one channel is designated to perform lateral accelerations in the vertical plane and the other in the direction perpendicular to it. An appropriate missile's guidance law generates the acceleration command for each channel subject to the saturation imposed by the maximum lift coefficient. In the present study two different differential games guidance laws are considered: (i) DGL/1 – derived using the simplified linear model [2], (ii) DGL/E – derived using the presented extended linear model.

**Simplified Example**

As noted before, the velocity and maneuverability of both missiles during the end-game is time-varying. Based on Figs. 2 & 3 two simplifying assumptions can be made:

(SA-1) The interception scenario is between an interceptor with a constant longitudinal acceleration [$\mathbf{a}_{xp}(t) = \mathbf{a}_{xp}$] and a constant speed reentering TBM [$\mathbf{a}_{xe}(t) = 0$].

(SA-2) The maneuverability of the interceptor is constant, while that of the evader is linearly time varying.

In the preliminary analysis described in [7] two elementary examples, using each of these assumptions separately, were presented. In this example a more realistic scenario, where both of these assumptions are simultaneously valid, is analyzed.

Based on simplifying assumption (SA-1) the pursuer's velocity can be expressed as

$$V_p(t) = V_{pf}\,(1 - \alpha t_{go}/\tau_P) \tag{65}$$

where $V_{pf}$ is the pursuer's final velocity and

$$\alpha = \mathbf{a}_{xp}\tau_p/V_{pf} \tag{66}$$

Based on (SA-2) the evader's maneuverability can be expressed as

$$\mathbf{a}_E^{max}(t) = \mathbf{a}_{Ef}^{max}\,[1-\beta t_{go}/\tau_P] \tag{67}$$

The zero effort miss distance of this simplified problem is

$$Z^{\alpha\beta} = Z^1 + \Delta Z^{\alpha\beta} \tag{68}$$

where $Z^1$ is the zero effort miss distance for the constant speed model (see Appendix) and

$$\Delta Z^{\alpha\beta} = -[III_P(t_{go})\tau_p^{\,2}x_3 + 0.5\alpha\, t_{go}^{\,2}V_{pf}\,x_5/\tau_p] \tag{69}$$

with

$$III_P(t_{go}) = \int_0^{t_{go}}\!\!\int\!\!\int \frac{\alpha e^{-\frac{\zeta}{\tau_P}}}{\tau_P^2\left(1-\alpha\dfrac{\zeta}{\tau_P}\right)}\,d\zeta d\xi d\varsigma \tag{70}$$

The state variables that affect the change of the *zero effort miss* distance are $x_3$ ($\mathbf{a}_p$) and $x_5$ ($\phi_p$) only. Using the new definition of (68) the optimal strategies of (40)

become

$$\mathbf{u}^* = \mathbf{v}^* = \text{sign}\,\{Z^{\alpha\beta}\} \tag{71}$$

and the resulting optimal trajectories are

$$\frac{dZ^{\alpha\beta}}{dt}^* = \Gamma^{\alpha\beta}(t_f,t)\cdot \text{sign}(Z^{\alpha\beta}) \tag{72}$$

where

$$\Gamma^{\alpha\beta}(t_f,t) = a_P^{max}\left[e^{-\frac{t_{go}}{\tau_P}} + \frac{t_{go}}{\tau_P} - 1 + III_P(\frac{t_{go}}{\tau_P})\right]\tau_P - \\ -a_{Ef}^{max}\left[e^{-\frac{t_{go}}{\tau_E}} + \frac{t_{go}}{\tau_E} - 1\right]\tau_E(1-\beta\frac{t_{go}}{\tau_P}) \tag{73}$$

It can be shown that this function corresponds to case 4. The non vanishing solution of the equation $\Gamma^{\alpha\beta} = 0$ (if it exists) provides $(t_{go})_s^{\alpha\beta} > 0$ and the value of the game in region $\boldsymbol{D_0}$ is

$$M_s^{\alpha\beta} = \int_0^{(t_{go})_s} \Gamma^{\alpha\beta} dt \tag{74}$$

The affect of the normalized parameters $\alpha$ and $\beta$ defined by (66) and (67), on the critical time and on the guaranteed normalized miss distance is shown in Figs. 9 and 10, respectively.

As can be seen from Fig. 10 the guaranteed miss distance decreases as $\alpha$ increases. The reason is that the velocity vector is generally not aligned with the line of sight and consequently a positive longitudinal acceleration ($\alpha > 0$) has a component normal to the LOS. This augments the pursuer maneuverability and results in smaller miss distances. An increase in $\beta$ results also in a decrease in the guaranteed miss distance since the effective maneuverability ratio during the end game is smaller than its final value used in (67).

The above outlined extended linear model leads to a substantial improvement in the homing accuracy in realistic scenarios with time varying missiles velocities and maneuverabilities. This is demonstrated by results of the three-dimensional nonlinear simulation shown in Figs. 11 and 12. In Fig. 11 the robust behavior of DGL/E is clearly seen. Moreover, the extended linear model provides a much more accurate prediction of the miss distance obtained by the three-dimensional nonlinear simulation, as shown in Fig. 13. The negligible differences confirm the validity of the model.

## Appendix: Game with Constant Maneuverability and Velocity

This game have served as a simplified linearized model for the terminal phase of intercepting a maneuvering target by a guided missile [8, 11]. The game solution is based on the assumptions that both players have constant velocities and the bounds on their lateral accelerations are also constant. Consequently, the pursuer/evader maneuverability ratio, defined as

$$\mu = a_P^{max} / a_E^{max} \tag{A-1}$$

is a fixed parameter of the game. It is also assumed that the interception takes place in a plane with small deviations from the initial line of sight. The equations of motion are written in Cartesian coordinates, where the X axis is aligned with the initial line of sight. The assumptions of constant speed and trajectory linearization allow solving the equation of motion in the X direction as a function of time-to-go. Therefore, only the equations of motion in the Y direction (perpendicular to the initial line of sight) remain to be solved.

If both players have first order dynamics [13], the game (called in the recent literature as DGL/1 and its variables will be denoted with the superscript 1) has 4 state variables of Eqs. (3-6). The "terminal projection" transformation leads to the definition of *the zero effort miss distance as*

$$Z^1(t) = x_1(t) + x_2(t)\, t_{go} + \Delta Z_E(t) - \Delta Z_P(t) \tag{A-2}$$

where

$$\Delta Z_E(t) = \tau_E^2 \left(e^{-\theta/\varepsilon} + \theta/\varepsilon - 1\right) x_4(t) \tag{A-3}$$

$$\Delta Z_p(t) = \tau_p^2 \left(e^{-\theta} + \theta - 1\right) x_3(t) \tag{A-4}$$

and $\theta$, $\varepsilon$ are normalized parameters defined by

$$\theta = (t_f - t)/\tau_P \tag{A-5}$$

$$\varepsilon = \tau_E / \tau_P \tag{A-6}$$

In order to obtain a more general solution the *normalized zero effort miss distance* is defined

$$\overline{Z^1} = \frac{Z^1}{a_E^{max} \tau_P^2} \tag{A-7}$$

The optimized normalized game dynamics is

$$\frac{d\overline{Z^1}^*}{dt} = \overline{\Gamma^1}(\theta, \mu, \varepsilon) \cdot \text{sign}(\overline{Z^1}) \qquad \text{(A-8)}$$

where

$$\overline{\Gamma}^1(\theta, \mu, \varepsilon) = \mu\,[e^{-\theta} + \theta - 1] - \varepsilon[e^{-\theta/\varepsilon} + \theta/\varepsilon - 1] \qquad \text{(A-9)}$$

The game space can have 5 different structures depending on the parameters $\mu$ and $\varepsilon$, as shown in Table A-1.

| | $\mu < 1$ | $\mu = 1$ | $\mu > 1$ |
|---|---|---|---|
| $\mu\varepsilon < 1$ | Case 1 (Fig. 4) | Case 1 (Fig. 4) | Case 4 (Fig. 7) |
| $\mu\varepsilon = 1$ | Case 1 (Fig. 4) | Case 2 (Fig. 5) | Case 3 (Fig. 6) |
| $\mu\varepsilon > 1$ | Case 5 (Fig. 8) | Case 3 (Fig. 6) | Case 3 (Fig. 6) |

**Table A-1. Conditions for various game solution structutes**

In all of these cases the *guaranteed normalized miss distance* in region $\mathcal{D}_1$ depends on the initial conditions, as well as on the parameters $\mu$ and $\varepsilon$. The region $\mathcal{D}_0$ exists only in cases 3-5. The *guaranteed normalized miss distance* for this entire region depends only on the parameters $\mu$ and $\varepsilon$.

$$\overline{M}_s = \mu(1-\varepsilon)(e^{-\theta_s^1} + \theta_s^1 - 1) - [(\mu-1)(\theta_s^1)^2]/2 \qquad \text{(A-10)}$$

where $\theta_s^1$ is the strictly positive solution of the equation $\overline{\Gamma}^1(\theta, \mu, \varepsilon) = 0$. In case 4 both $\theta_s^1$ and $\overline{M}_s$ *are* identically zero.

# PART 2

# SUMMARY
# OF THE MULTI-YEAR INVESTIGATION

## Objectives

The objective of the research contract, planned for two years of activity, was the evaluation and development of interceptor guidance laws against highly maneuvering autonomous unmanned flying vehicles. The effort was aimed at understanding how key parameters in the models of the interceptor missile and of the target affect the outcome of an engagement. In particular, the following questions were addressed:

a) "Are the conclusions of earlier studies, derived on the basis of a simplified linear mathematical model, valid for the *real world problem* of intercepting highly maneuvering autonomous unmanned flying vehicles expected in the future?"

b) "To what extent can linear guidance theory be used to predict the **guaranteed miss distance** in an actual *real world* engagement between a guided missile and its highly maneuverable target?"

In order to answer these questions, the investigation effort started with two detailed parametric simulation studies. In the first Interim Technical Report the results of nonlinear three-dimensional point-mass simulations of a theatre missile defense (TMD) scenario were compared to the predictions of linear guidance theory. The second Technical Report presented a similar analysis of a cruise missile defense scenario, which has very different characteristics. In particular the altitude of the interception end-game is constant and the speed variations are generally minor.

The characteristics of these two scenarios were selected in order to isolate the affect of the nonlinear kinematics from those of speed and altitude variations. For the sake of having a better insight, measurement noise and the associated estimation problem were not included in the simulations. Several guidance laws were compared in both studies. For those guidance laws that required explicit knowledge of the target acceleration, it was assumed that this information is obtained with a fixed time delay representing the convergence time of the (not simulated) estimator. This delay was one of the parameters of the investigation.

## Results

In spite of the great differences between the two simulated scenarios, both studies confirmed that the major conclusions of earlier studies, based on linear guidance theory, remain valid in a realistic environment:

1. The currently available guidance laws and estimation techniques cannot guarantee a "hit-to-kill" accuracy in the interception of highly maneuvering tactical ballistic or cruise missile that are expected in the future. The main reasons for this failure are insufficient maneuverability advantage and inherent delay in estimating target maneuvers.

2. Guidance laws derived using differential game theory provide an improved **guaranteed** (robust) homing accuracy compared to currently used "modern" guidance laws based on optimal control.

Moreover, the two simulation studies created an enhanced understanding of the affects of some key parameters on the outcome of a missile/target engagement and also indicated the limitations of the currently existing theory. The sensitivity trends of the **guaranteed miss distance** with respect to the parameters of the interception in a realistic environment were found to be similar, but **not identical**, to the trends predicted by a linear model. In spite of the similarity in trends, it was realized that currently existing linear guidance theory can not be used to predict the miss distance in an actual *real world* missile/target engagement. A major reason for the differences has been identified as the assumptions of the linear model on constant velocities and constant lateral acceleration bounds. The affects of nonlinear kinematics in the TMD interception scenario were found negligible.

By isolating the affect of the nonlinear kinematics, it was found that most of the discrepancies, associated with the variable speed and maneuverability vanish in the cruise missile defense scenario. In the maneuvering end-game of the cruise missile defense scenario, characterized by high turning rates, the affect of nonlinear kinematics cannot be neglected. The end-game maneuvers executed by both missiles create large angular deviations from the initial interception geometry that invalidate the linearized kinematical model used for guidance law development. Therefore, it is absolutely necessary for an effective guidance, to assure that in the zero effort miss distance expressions of the guidance laws the acceleration components normal to the line of sight are used, as implied by linear guidance theory. This very important guidance law modification is not always implemented in existing missile systems. The same is needed for a meaningful comparison between the results of nonlinear and linear simulations. The nonlinear simulations confirm that in many cases the maximum miss distance is only about 2/3 of the value obtained with linearized kinematics. This is due to the reduced lateral acceleration component of the cruise missile normal to the line of sight (maximum aspect angle of about $40^0$).

Based on these results the direction to be taken in the next phase of the investigation was to extend currently used linear guidance models to allow for variable speed and maneuverability, in order to yield guidance law modification and improved homing accuracy. This effort was successfully completed, as it is described in the first part of this report. Moreover, the extended linear guidance model allowed predicting the miss distance in an actual, real world, missile/target engagement more accurately.

## Conclusions

By comparing the objectives and the results of the investigation, as outlined above, it can be clearly seen that the objectives were fully reached within the limited frame selected from the outset. By restricting the investigation from the outset in noise free scenarios, it has been easier to understand how key parameters in the interceptor missile and the target models affect the outcome of an engagement. The limitations of the frequently used linear guidance theory in a noise free, but otherwise realistic

interception scenarios have been identified. The extension of a time-varying model within the frame of linear differential game theory has become an important step towards the development of a new guidance law for an efficient and satisfactory defense against highly maneuvering tactical ballistic or cruise missiles expected in the future. The separation between deterministic parameters allowed a very detailed parametric sensitivity analysis with an affordable computational effort.

It has to be admitted, however, that the deterministic analysis (detailed and profound, as it could be) does not present the complete picture. It is well known, that the accuracy of any guidance system is limited by the errors of the estimation process, which is necessary in realistic environment with noise corrupted measurements. In two recent works [14, 15] (performed outside the AFOSR sponsored effort) improved guidance performance was achieved by proper selection of the estimation process. There is another basic issue to be considered in this respect. The common practice in guidance system design has been to use the estimated variables of the stochastic interception scenario in the perfect information guidance law. This practice is based on the assumption that the stochastic guidance problem possesses the certainty equivalence property. Moreover, it also assumes that the optimal guidance problem is also separable (i.e. that the optimal estimation algorithm does not depend on the optimal guidance law and vice versa [16]. Since these assumptions are not valid for realistic interception scenarios against randomly maneuvering targets, this approach is clearly not optimal in a rigorous sense. It was suggested [17] that for such cases a separate design of the estimator is allowed, but the optimization of the control law has to be based on the probability density function of the estimated state variables. An example in this direction has been analyzed within the frame of a recent BMDO contract [18]. In this example the it was demonstrated that for any given estimator the delay induced by the non ideal convergence of the estimation process of the target maneuver can be compensated, leading to an significant improvement of the guaranteed guidance performance.

The success in deterministic analysis and the recent results dealing with estimation indicate the need to integrate these two elements in the development of a new approach of interceptor guidance, which takes into account not only time varying parameters, but also the limitations of the *available* estimation techniques. In this context, optimizing the estimation process has to be the first step in the overall guidance/estimation improvement strategy. These conclusions outline a new, very ambitious research effort aimed to achieve an efficient and satisfactory defense against highly maneuvering tactical ballistic or cruise missiles expected in the future,

## References


1. Shinar, J., Shima, T. and Kebke, A. "Evaluation of Guidance Laws for the Interception of Highly Maneuvering Targets - Comparison to Linear Analysis", AIAA 11th Multinational Conference on Theater Missile Defense, Monterey CA, June 1998.
2. Shinar, J., Shima, T. and Kebke, A., "On the Validity of Linearized Analysis in the Interception of Reentry Vehicles", *Proceedings of the AIAA Guidance Navigation and Control Conference*, Boston, MA, Aug. 1998, pp. 1050-1060.
3. Lee, G. F. K. "Estimation of the Time-to-Go Parameter for Air-to-Air", *Journal of Guidance Control and Dynamics,* Vol. 8, No. 2, 1985, pp. 262-266
4. Gazit, R. and Gutman, S. "Development of Guidance Laws for a Variable-Speed Missile", *Dynamics and Control,* Vol. 1, No. 2, 1991, pp. 177-198.
5. Baba, Y., Takehira, T. and Takano, H. "New Guidance Law for a Missile with Varying Velocity", *Proceedings of the AIAA Guidance Navigation and Control Conference*, Washington, D.C., 1994, pp. 207-215 (AIAA CP94-3565).
6. Cho, H., Ryoo, C.K. and Tahk, M. J. "Closed-Form Optimal Guidance Law for Missiles of Time-Varying Velocity", *Journal of Guidance Control and Dynamics,* Vol. 19, No. 5, 1996, pp. 1017-1022.
7. Shima, T. and Shinar, J. "On the Extension of Linear Pursuit - Evasion Game Models Applied for Interception Analysis", *Proceedings of the 39th Israel Annual Conference on Aerospace Sciences*, Tel-Aviv and Haifa, Israel, Feb. 1999, pp. 142-152.
8. Gutman, S. and Leitmann, G. "Optimal Strategies in the Neighborhood of a Collision Course", *AIAA Journal,* Vol.14, No. 9., 1976, pp.1210-1212.
9. Gutman, S., "On Optimal Guidance for Homing Missiles", *Journal of Guidance and Control* Vol. 3, No. 4, 1979, pp. 296-300.
10. Shinar, J. and Zarkh, M. "Interception of Maneuvering Tactical Ballistic Missiles in the Atmosphere", *Proceedings of the 19th ICAS Congress and AIAA Aircraft Systems Conference,* Anaheim, CA, Sept. 1994, pp. 1354-1363.
11. Shinar, J. and Steinberg, D., "Analysis of Optimal Evasive Maneuvers Based on a Linearized Two-Dimensional Kinematic Model", *Journal of Aircraft,* Vol. 14, No. 8, 1977, pp. 795-802.
12. Shinar, J., Rotsztein, Y. and Bezner, A., "Analysis of Three-Dimensional Optimal Evasion with Linearized Kinematics", *Journal of Guidance and Control,* Vol. 2, No. 5, 1979, pp. 353-360.
13. Shinar, J., "Solution Techniques for Realistic Pursuit-Evasion Games" in *Advances in Control and Dynamic Systems,* Vol. 17, Academic Press, NY 1981, pp. 63-124.
14. Oshman Y., Shinar J. and Avrashi Weizman S., "Using a Multiple Model Adaptive Estimator in a Random Evasion Missile/Aircraft Encounter", *Proceedings of the AIAA Guidance, Navigation and Control Conference*, Portland, OR, Aug. 1999, pp. 1017-1027.
15. Shima T., Oshman Y. and Shinar J., "Intercepting Maneuvering Ballistic Missiles Using an Efficient Multiple Model Adaptive Estimator", *Proceedings of the 40th Israel Annual Conference on Aerospace Sciences*, Feb. 2000, pp. 199-210.
16. Stengel, R. F., *"Stochastic Optimal Control"*, John Wiley & Sons, New York, 1986
17. Witsenhausen, H. S., "Separation of Estimation and Control for Discrete Time Systems," *Proceedings* of the IEEE, Vol. 59, No. 11, Nov. 1971, pp. 1557-1566.
18. Shinar J. and Shima T., "Robust Missile Guidance Law against Highly Maneuvering Targets", *Proceedings of the 7th IEEE Mediterranean Conference on Control and Automation*, Haifa, Israel, June 1999, pp. 1548-1572.

## List of figures

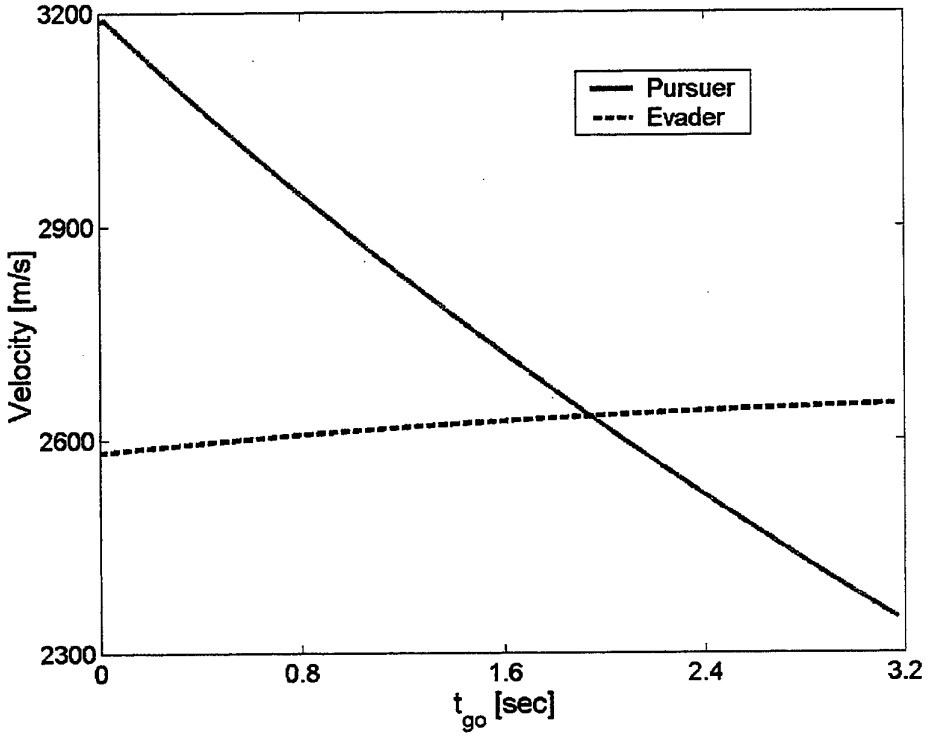


Fig. 1 End-game velocity profiles.

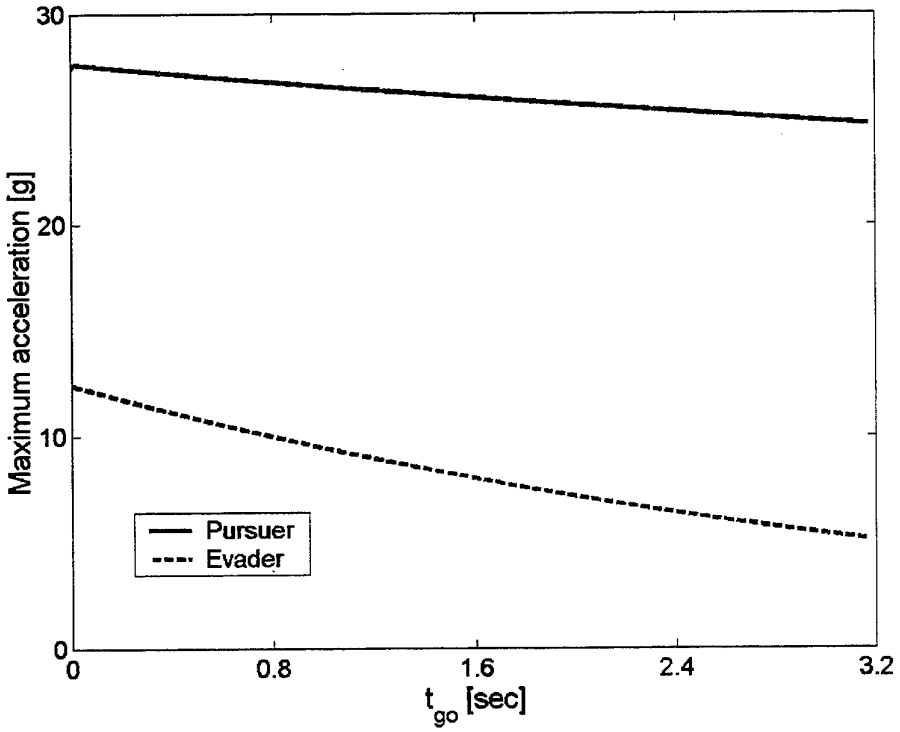


Fig. 2 Time histories of end-game maneuverability.

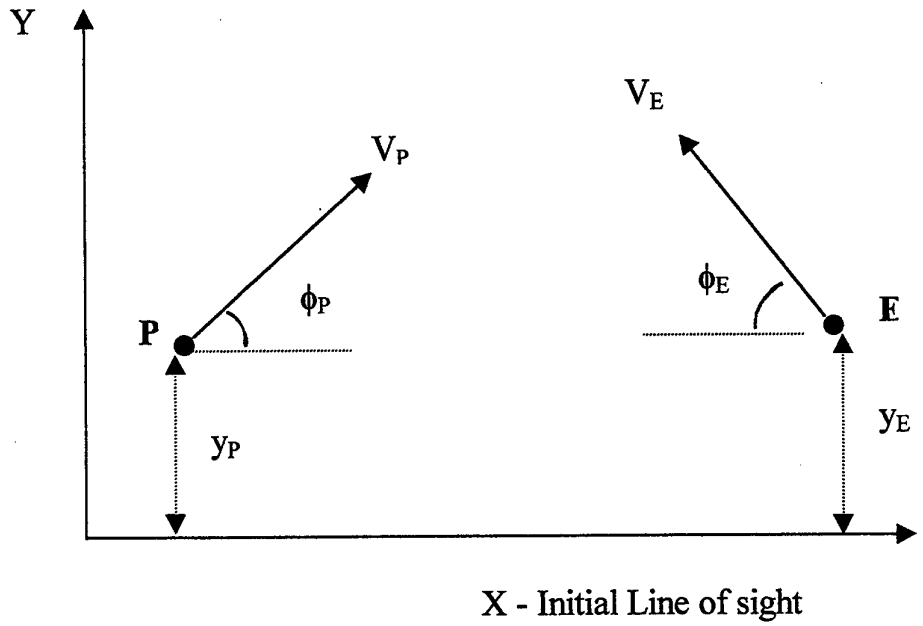


Fig.3 Planar end-game geometry.

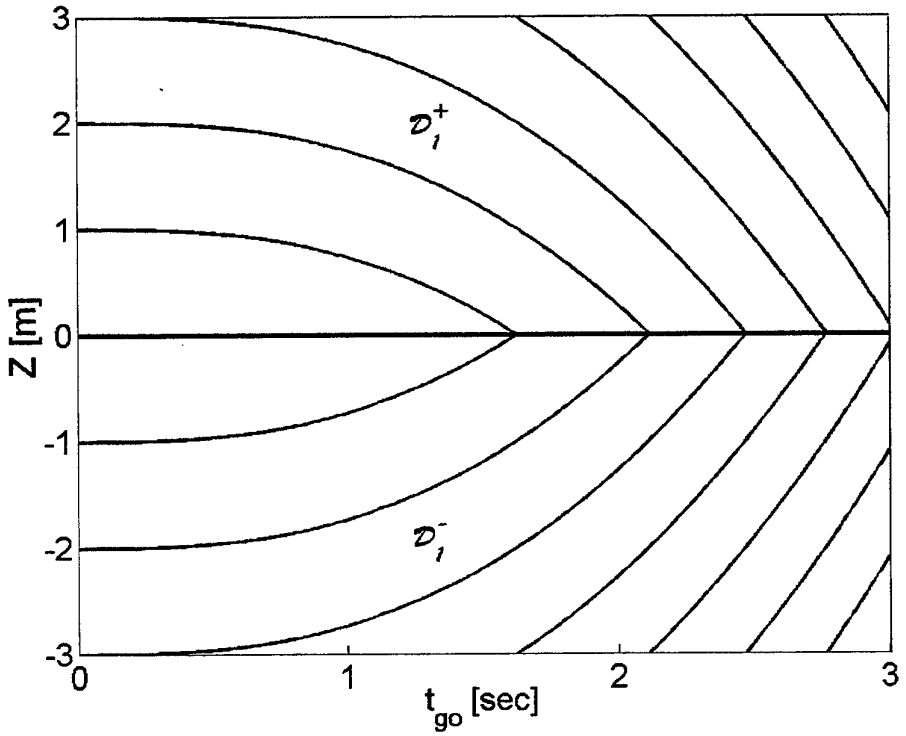


Fig. 4 Game space decomposition for Case 1($\mu < 1$, $\mu\varepsilon \leq 1$).

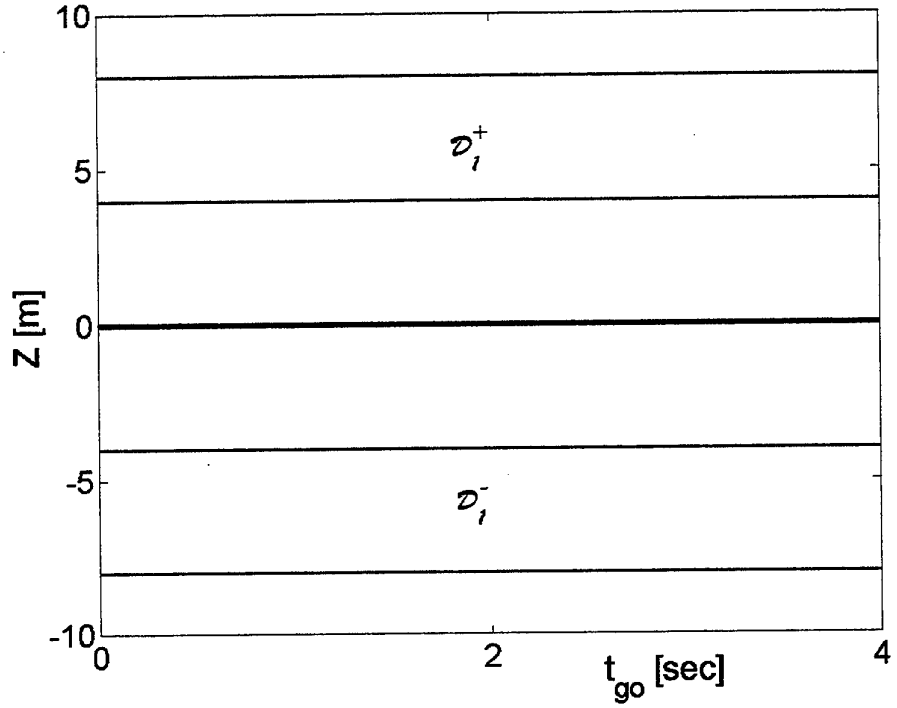


Fig. 5 Game space decomposition for Case 2 ($\mu = 1$, $\mu\varepsilon = 1$).

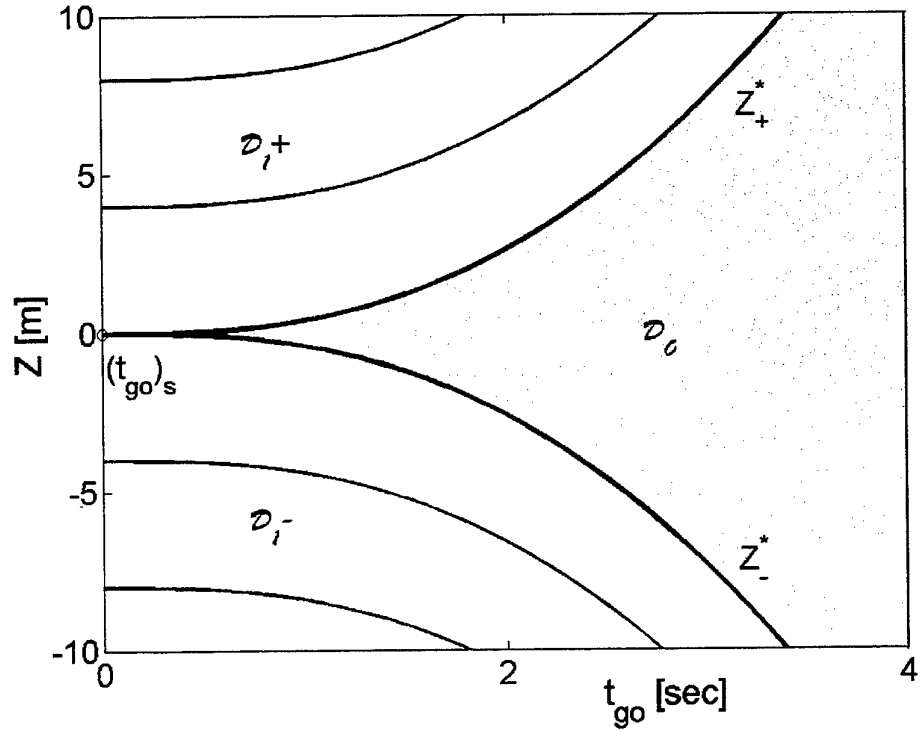


Fig. 6 Game space decomposition for Case 3 ($\mu > 1$, $\mu\varepsilon \geq 1$).

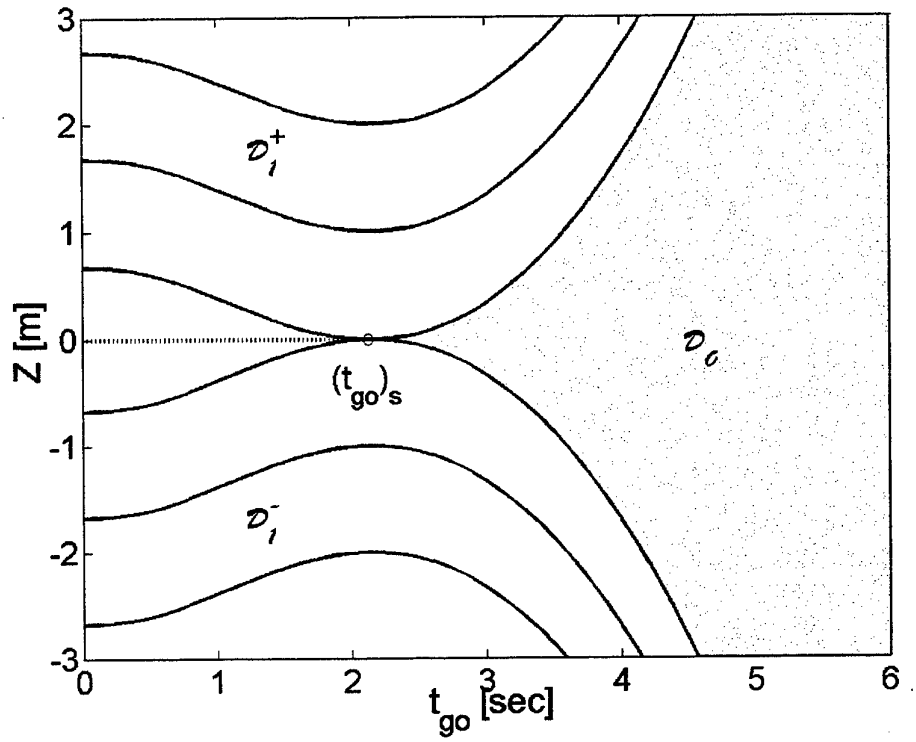


Fig. 7 Game space decomposition for Case 4 ($\mu > 1$, $\mu\varepsilon < 1$).

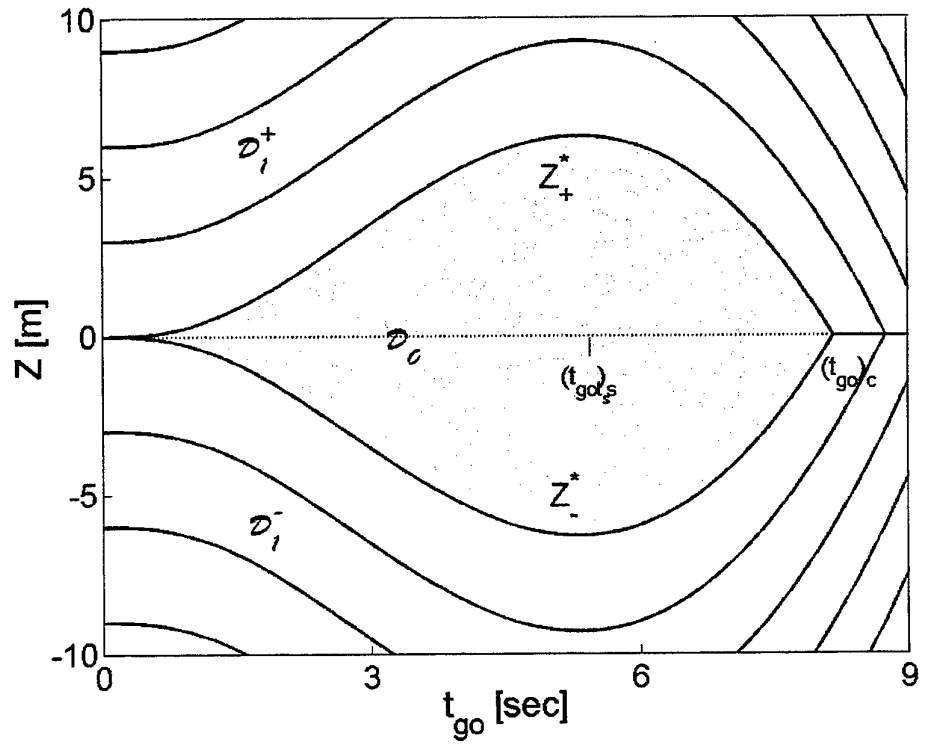


Fig. 8 Game space decomposition for Case 5 ($\mu < 1$, $\mu\varepsilon > 1$).

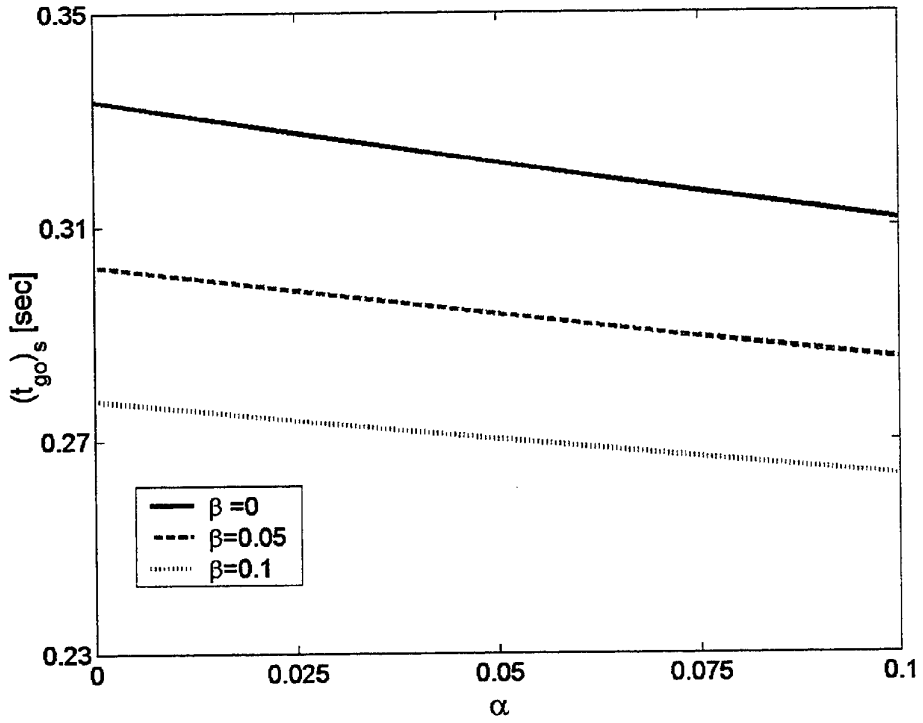


Fig. 9 Critical time-to-go. $\mu_f = 2.19, (a_P^{max} = 27.5g), \varepsilon = 0.25, (\tau_E = 0.1\text{sec})$

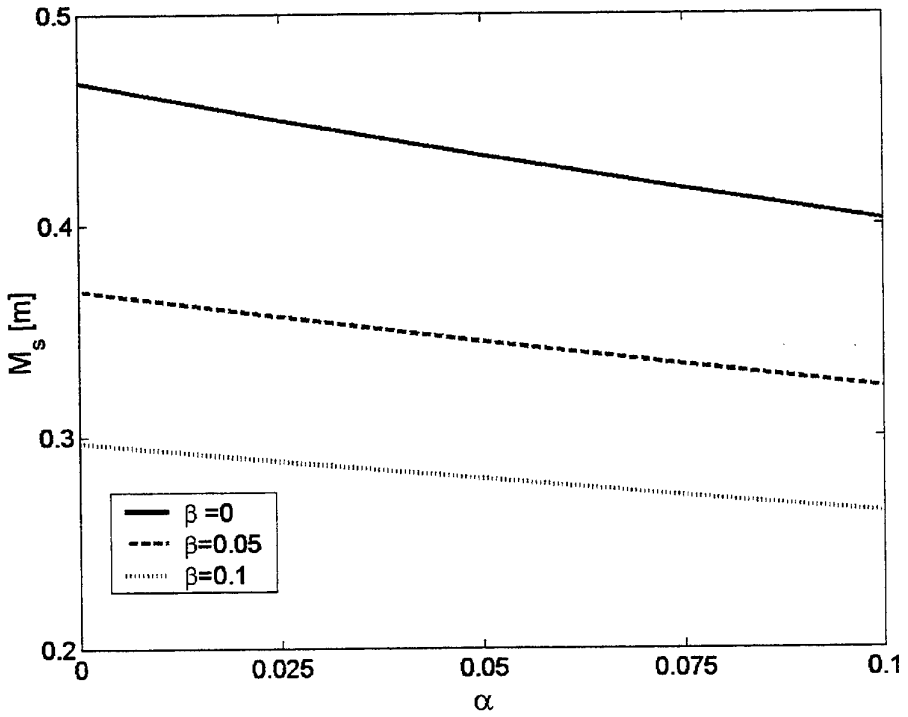


Fig. 10 Guaranteed miss distance. $\mu_f = 2.19, (a_P^{max} = 27.5g), \varepsilon = 0.25, (\tau_E = 0.1\text{sec})$

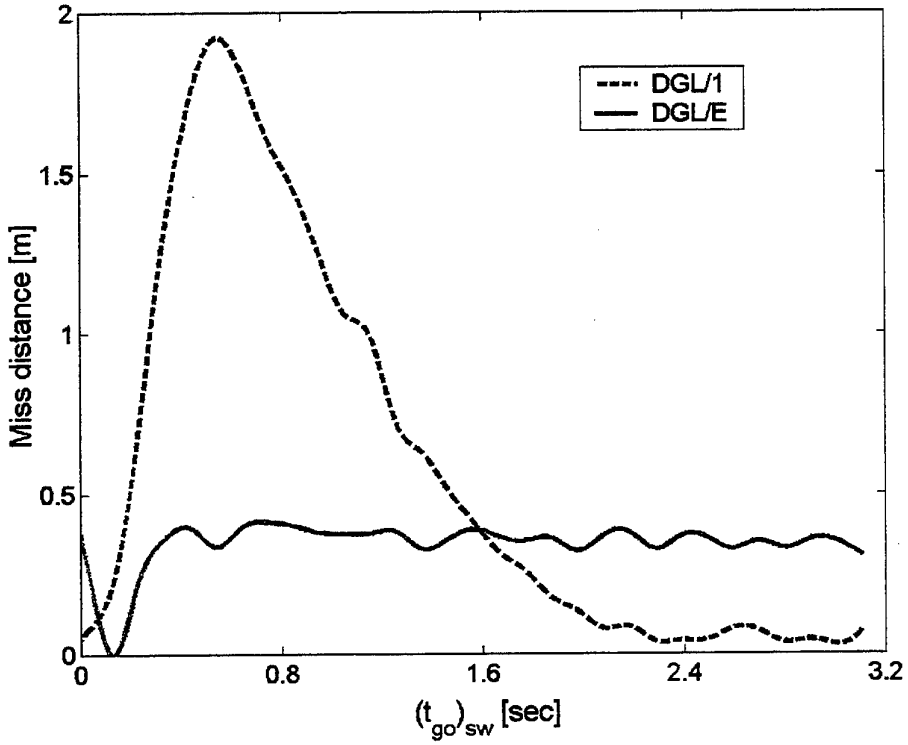


Fig. 11 Miss distance vs. $(t_{go})_{sw}$ . $\mu_f = 2.19, (a_P^{max} = 27.5g), \varepsilon = 0.25, (\tau_E = 0.1\text{sec})$
$\alpha$=0.034, $\beta$=0.074

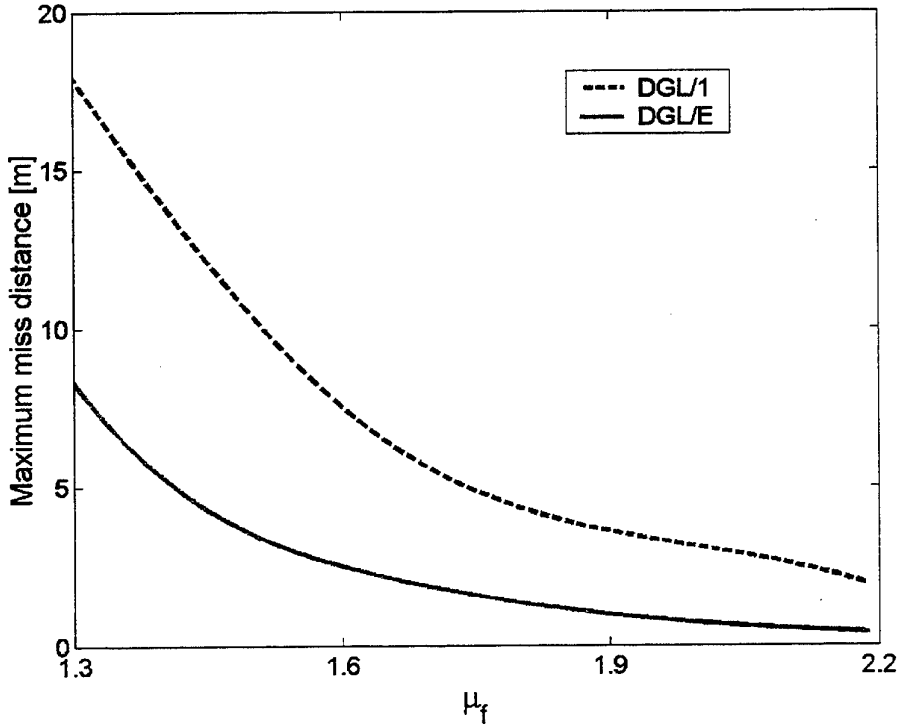


Fig. 12 Maximum miss distance vs. final maneuverability ratio
$a_P^{max} = 27.5g, \varepsilon = 0.25, (\tau_E = 0.1\text{sec}), \alpha = 0.034, \beta = 0.074$

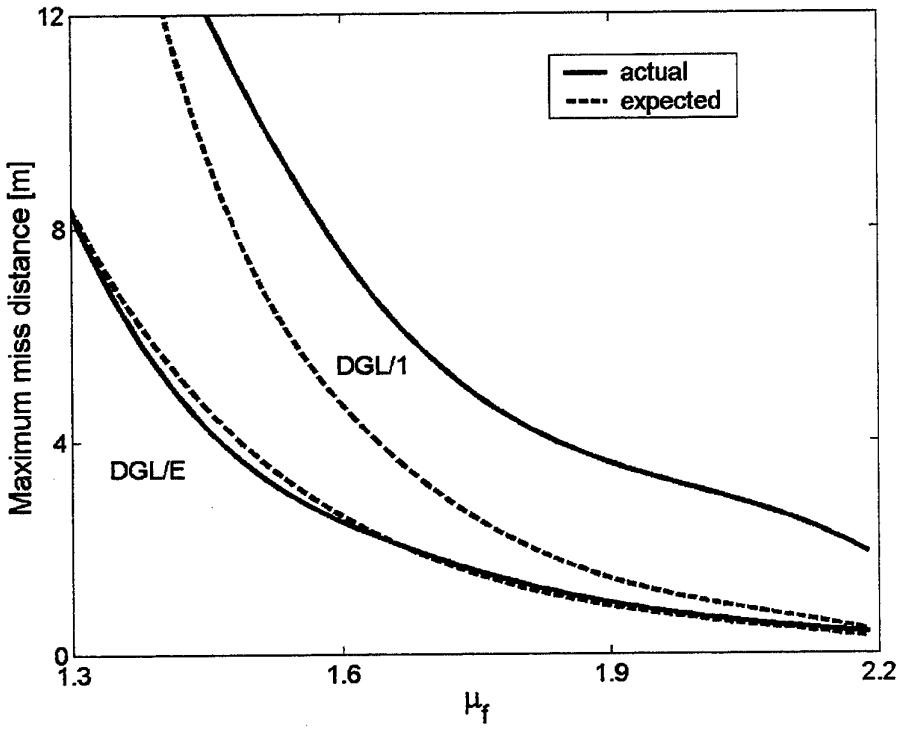


Fig. 13 Expected vs. actual miss distances for DGL/1 and DGL/E.
$a_P^{max} = 27.5g, \varepsilon = 0.25, (\tau_E = 0.1\text{sec}), \alpha = 0.034, \beta = 0.074$